JOURNAL OF DYNAMICS AND CONTROL

VOLUME 8 ISSUE 10

IN-SILICO SYNTHESIS: PREDICTING THE ACTIVE SITES OF GUANINE AND PHENYLALANINE TO CREATE A NOVEL MOLECULE THROUGH GAUSSIAN SIMULATION

Shanmugasundari. M[1], Vijaya. P.[2]

[1]Research scholar (Reg. No. 20211172032001),
[2]Assistant Professor,
Department of Chemistry, Rani Anna Government College for Women, Tirunelveli-8, (Affiliated to Manonmaniam Sundaranar University, Tirunelveli - 627 012), India.

IN-SILICO SYNTHESIS: PREDICTING THE ACTIVE SITES OF GUANINE AND PHENYLALANINE TO CREATE A NOVEL MOLECULE THROUGH GAUSSIAN SIMULATION

Shanmugasundari. M[1*], Vijaya. P.[2]

[1]Research scholar (Reg. No. 20211172032001), [2]Assistant Professor,
Department of Chemistry, Rani Anna Government College for Women, Tirunelveli-8,
(Affiliated to Manonmaniam Sundaranar University, Tirunelveli 627 012, India)
[1]shanmugasundarichemistry@gmail.com, [2]racchemonlineclass@gmail.com
[*]ORCID: 0009-0001-0531-5859

Corresponding Author

ABSTRACT: In this study, we employ Gaussian software to perform a comprehensive theoretical investigation of the reaction between guanine and phenylalanine. The research primarily focuses on the Fukui function calculations to assess the nucleophilic and electrophilic reactivity of the reactants. Geometry optimization is conducted to determine the most stable structures of the reaction products. The theoretical evaluation of the product is extended to include Fourier-transform infrared spectroscopy (FTIR) and nuclear magnetic resonance (NMR) analysis, which provide insights into their vibrational modes and structural characteristics. Natural bond orbital (NBO) analysis sheds light on the electronic structure, while polarizability studies, AIM (atoms in molecules) analysis, and multiwave function analysis offer a deeper understanding of the electronic distribution and interaction patterns. The study also incorporates molecular electrostatic potential (MEP) and frontier molecular orbital (FMO) analyses to explore the electronic properties and reactivity profiles of the products. This comprehensive theoretical approach not only elucidates the reaction mechanisms but also provides valuable information on the stability and reactivity of the product, contributing to a more profound understanding of the guanine-phenylalanine interaction.

KEYWORDS: ***DFT, Pass Bio-activity, AIM, Multiwave Function Analysis***

1. Introduction

Theoretical and computational chemistry provides a robust framework for understanding the intricate mechanisms of chemical reactions and the properties of molecules. In this study, we focus on the theoretical investigation of a reaction between guanine and phenylalanine, leveraging advanced computational methods to gain insights into the molecular interactions and product characteristics. Guanine [1-2], a fundamental nucleobase in DNA, and phenylalanine [3-5], an essential amino acid, are both pivotal in biochemical processes. There are numerous guanine derivatives that have been synthesized and studied for their medicinal properties. These derivatives often exhibit enhanced pharmacological effects compared to guanine itself. They have been explored in the treatment of various diseases, including cancer, viral infections, and neurodegenerative disorders [6–13]. Their interaction and reaction products are of significant interest in understanding biomolecular dynamics and interactions. Gaussian software, a leading computational chemistry tool, is employed to perform detailed theoretical analyses. The Fukui function calculation [14], a crucial component of this study, helps elucidate the nucleophilic and electrophilic reactivity of the guanine and phenylalanine molecules. Geometry optimization of the reaction products is carried out to determine their stable conformations. Additionally, various theoretical spectroscopy techniques such as FTIR (fourier-transform infrared spectroscopy), NMR (nuclear magnetic resonance) spectroscopy, NBO (natural bond orbital) analysis, polarizability studies, AIM (atoms in molecules) analysis, and multiwave function analysis are used to thoroughly characterize the reaction product of (PG). The molecular electrostatic potential (MEP) and frontier molecular orbital (FMO) analysis further provide insights into the electronic properties and reactivity of the compounds.

2. Computational techniques

The Gaussian 03W software package is employed for all density functional theory (DFT) studies. The designed structure was optimized for geometry at the minimum energy by the B3LYP/DFT 6-31G (d, p) basis set.
The optimized structure is subjected to frequency calculation using the before specified basis set, with the unscaled frequency converted to the scaled frequency using a scaling factor of 0.9614. The potential energy difference (PED)% of the molecule was achieved using the Veda4 program [15].
The optimized structure is also subjected to NMR calculations using the 6-311+G (2d,p) basis set and chloroform as the solvent. Polarizability and natural bond orbital computations [16] were carried out using the 6-31G (d,p) basis set. The molecule's dipole moment (μ), polarizability <α>, and hyperpolarizability βtot, which are calculated as follows,

$$\mu = (\mu_x^2 + \mu_y^2 + \mu_z^2)^{1/2} \quad (1)$$
$$<\alpha> = 1/3\,(\alpha_{xx} + \alpha_{yy} + \alpha_{zz}) \quad (2)$$
$$\beta_{tot} = [(\beta_{xxx} + \beta_{xyy} + \beta_{xzz})^2 + (\beta_{yyy} + \beta_{yzz} + \beta_{xxy})^2 + (\beta_{zzz} + \beta_{xxz} + \beta_{yyz})^2]^{1/2} \quad (3)$$

The compound's highest occupied molecular orbital (HOMO), lowest unoccupied molecular orbital (LUMO), and molecular electrostatic potential (MEP) surfaces [17] are visualized. The electronic properties of the compounds' band gap energy, electronegativity (χ), chemical hardness (η), softness (S), chemical potential (σ), and globalphilicity (ω) values can be used to calculate as follows:

$$\eta = ½\,[E_L - E_H] = [I - A]/2 \quad (4)$$
$$S = 1/\eta \quad (5)$$
$$\sigma = -\,(E_H + E_L)/2 \quad (6)$$
$$\chi = -\,E_L \quad (7)$$
$$\omega = \sigma^2/2\,\eta \quad (8)$$

The AIMALL software [18] is utilized to determine the atoms in molecules (AIM), while the Multiwavefunction Analyzer is used to demonstrate the AIM computation results. The fukui functions of three different population analysis methods, namely Mulliken population (MCA), natural population (NCA), and Hirshfeld population (HCA), have been employed. Additionally, separate single-point energy calculations have been performed on electronic systems with N-1, N, and N+1 electrons. The critical atomic sites of the molecule were calculated using the following formulas:

$$f_k^+ = q^{N+1} - q^N \quad (9)$$
$$f_k^- = q^N - q^{N-1} \quad (10)$$
$$\Delta f = f_k^+ - f_k^- \quad (11)$$

$\Delta f > 0$, the site is preferred by nucleophilic attack and $\Delta f < 0$, the site is preferred by electrophilic attack.

3. Result and discussion

3.1. Conformational analysis

The molecules guanine and phenylalanine are separately optimized by the DFT method using the B3LYP/6-31G (d, p) method. Then the conformational analysis of PG is done in two ways. The one is fukui function (Δf) calculations, and another one is heat of formation (ΔHF). The nearby reactivity descriptors like fukui capacities and double descriptors are determined utilizing Mulliken population (MCA), Natural population (NCA), and Hirshfeld population (HCA), and free single-point energy estimations have been made on N-1, N and N+1 electronic frameworks (where N =

78 and N = 88, the absolute number of electrons in guanine and phenylalanine, respectively) with the same sub-atomic math (without any primary changes in the N-1, N and N+1 electronic frameworks) at B3LYP/6-31G+(d,p) level. For the calculation of fukui function (Δf), there is a possible reaction between guanine N11 (Δf = 0.046861) and phenylalanine O10 (Δf = -0.040263) by eliminating the H2O molecule. Because guanine (**Figure 1**) N11 is favorable for nucleophilic attack while phenylalanine (**Figure 2**) O10 is favorable for electrophilic attack. The fukui function (Δf) calculated table of guanine and phenylalanine is shown in the below **Table 1** and **Table 2**.

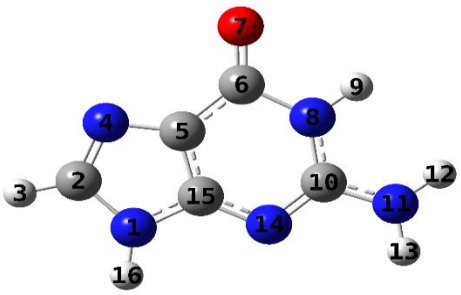

GUANINE
HF = -542.5642075 a.u.
(Figure 1)

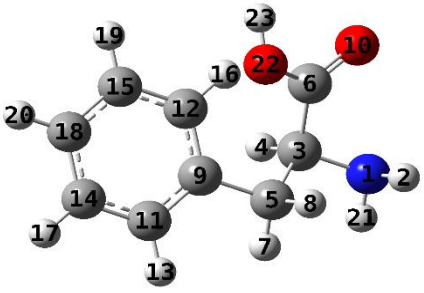

PHENYLALANINE
HF = -554.8120496 a.u.
(Figure 2)

Table 1. Fukui function calculation of Guanine based on Hirshfeld charge analysis (HCA)

Atomic site	q^N	q^{N+1}	q^{N-1}	f_k^-	f_k^+	**Δf**
N1	-0.049659	-0.089771	-0.012806	-0.036853	-0.040112	**-0.003259**
C2	0.040096	-0.062136	0.152821	-0.112725	-0.102232	0.010493
N4	-0.183174	-0.272808	-0.111796	-0.071378	-0.089634	-0.018256
C5	-0.03758	-0.070261	0.061538	-0.099118	-0.032681	0.066437
C6	0.146051	-0.003605	0.187513	-0.041462	-0.149656	-0.108194
O7	-0.300063	-0.457278	-0.169999	-0.130064	-0.157215	-0.027151
N8	-0.072267	-0.114454	-0.048188	-0.024079	-0.042187	-0.018108
C10	0.151313	0.116148	0.201886	-0.050573	-0.035165	0.015408
N11	-0.145251	-0.18232	-0.061321	-0.08393	-0.037069	0.046861
N14	-0.237437	-0.296576	-0.135388	-0.102049	-0.059139	0.04291
C15	0.05913	-0.013152	0.119716	-0.060586	-0.072282	-0.011696

Table 2. Fukui function calculation of phenylalanine based on Hirshfeld charge analysis (HCA)

Atomic site	q^N	q^{N+1}	q^{N-1}	f_k^-	f_k^+	**Δf**
N1	-0.212808	-0.233652	-0.057781	-0.155027	-0.020844	0.134183
C3	0.017376	-0.001141	0.047263	-0.029887	-0.018517	0.01137
C5	-0.052595	-0.073761	-0.019806	-0.032789	-0.021166	0.011623
C6	0.205495	0.122795	0.217709	-0.012214	-0.0827	-0.070486
C9	-0.001085	-0.066235	0.047116	-0.048201	-0.06515	-0.016949
O10	-0.271094	-0.362935	-0.219516	-0.051578	-0.091841	**-0.040263**
C11	-0.047417	-0.082245	-0.019819	-0.027598	-0.034828	-0.00723
C12	-0.045312	-0.123564	0.014722	-0.060034	-0.078252	-0.018218
C14	-0.041983	-0.123848	0.021451	-0.063434	-0.081865	-0.018431
C15	-0.040817	-0.084988	-0.001451	-0.039366	-0.044171	-0.004805
C18	-0.04311	-0.137328	0.047489	-0.090599	-0.094218	-0.003619
O22	-0.16774	-0.213634	-0.141108	-0.026632	-0.045894	-0.019262

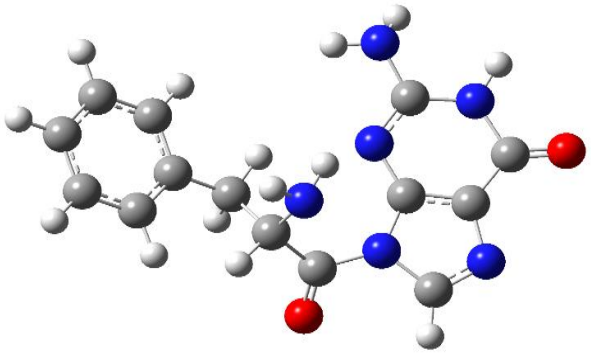

Figure 3. PG (conformer 1) HF = -1020.932 a.u

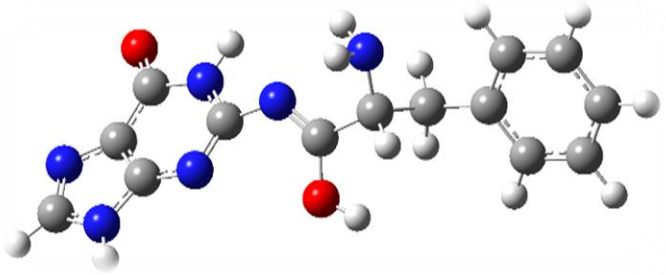

Figure 4. PG (conformer 2) HF = -1020.920 a.u

Two conformers, conformers 1 and 2 (**Figure 3** and **Figure 4**), are designed and subjected to optimization using the B3LYP/6-31G (d, p) basis set. From the energies derived from the output files, it is concluded that conformer 1 with minimum energy -1020.93 a.u is the ground state minimum energy conformer of PG. The scheme is represented in **Scheme 1**. This optimized conformer 1 is subjected to further computational analysis. The minimum energy conformer 1's structure of PG is shown in **Figure 5** with the labelling, and the selected parameters of bond length, bond angle, and torsional angle of the optimized geometry of PG are presented in **Table 3**.

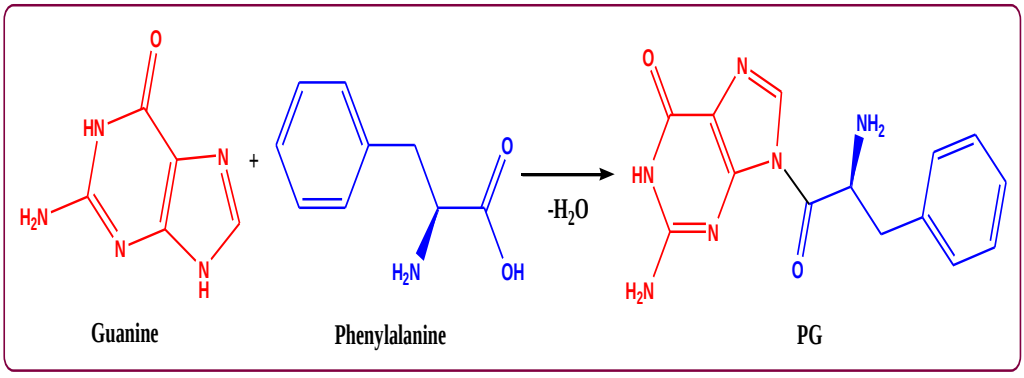

Scheme 1. **Systematic representation of the reaction between guanine and phenylalanine**

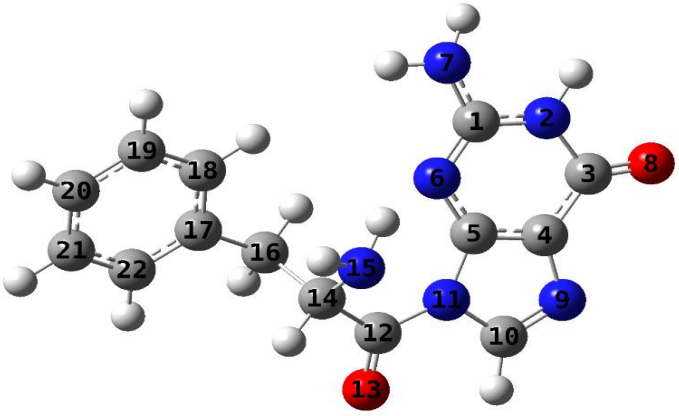

(ΔHF = -1020.932978 a.u)

Figure 5. Numbering adopted in the present study of PG

Table 3. Selected geometric parameters Bond Length (Å), Bond angle (º) and Torsion angle (º) of the optimized PG computed by DFT method (B3LYP/6 – 31G(d,p))

Bond	**Bond length (Å)**	**Bonds**	**Bond angle (O)**
C1-N7	1.37	C18-C17-C16	121.1
N7-H7A	1.01	C14-C16-C17	111.7
N7-H7B	1.01	C16-C14-N15	117.4
N2-H2	1.01	C14-N15-H15B	109.2
C3-O8	1.21	C14-N15-H15A	110.0
C10-H10	1.07	N15-C14-C12	111.7
N11-C12	1.43	C14-C12-O13	121.1
C12-013	1.21	N11-C12-C14	121.2
C12-C14	1.53	N11-C12-O13	117.5
C14-H14	1.09	C17-C16-H16A	110.5
C14-N15	1.46	C17-C16-H16B	109.7
N15-H15A	1.02	C12-C14-H14	46.8
N15-H15B	1.01	C10-N11-C12	120.2
C14-C16	1.56	N11-C10-H10	119.6
C16-H16A	1.09	N2-C3-O8	119.3
C16-H16B	1.09	H2-N2-C3	113.4
C16-C17	1.51	H2-N2-C1	120.4
-	-	N7-C1-N7	117.2
-	-	C1-N7-H7A	118.0
-	-	C1-N7-H7B	113.9
-	-	N7-C1-N6	119.4
-	-	O8-C3-C4	131.1
Bonds	**Torsion angle (O)**	**Bonds**	**Torsion angle (O)**
H2-N2-C1-N7	0.6	C12-C14-N15-H15A	82.15
H2-N2-C3-O8	-3.03	C12-C14-N15-H15B	-159.35
N2-C1-N7-H7A	29.5	N11-C12-C14-C16	85.4
N2-C1-N7-H7B	168.1	C12-C14-C16-C17	167.2
C6-C1-N7-H7A	-152.7	N15-C14-C16-H16A	58.95
C6-C1-N7-H7B	-14.1	N15-C14-C16-H16B	175.75
C12-N11-C10-H10	-1.3	C22-C17-C16-H16A	-31.98
013-C12-N11-C10	-11.7	C22-C17-C16-H16B	-150.7
O13-C12-C14-H14	18.2	C14-C16-C17-C22	89.2
O13-C12-C14-N15	132.6	C14-C16-C17-C18	-88.7

3.2. IR frequency examinations

The compound PG (PG) comprises of 36 atoms ($C_{28}N_6O_2$) and henceforth 102 normal modes of vibrations (35 stretching modes, 34 bending modes, 33 torsion modes, and 27 CH modes). The compound possesses C1 symmetry. All modes are IR active. The hypothetical vibrational spectra of PG have been computed by utilizing the DFT method with a 6-31G (d, p) basis set. The determined IR frequencies are scaled by a factor of 0.9614. The hypothetical IR vibrational spectra are interpreted through Potential Energy Distribution (PED%) computation utilizing the Vibrational Energy Distribution Analysis (VEDA) program. The normal modes of the hypothetical IR frequencies are pictured and validated with the assistance of the Gauss View 5.0 representation program. The IR spectrum is displayed in **Figure 6**. The normal modes are provided in decreasing order of wavenumbers in **Table 4**. None of the computed vibrational IR frequencies have any negative values, inferring that the optimized conformer is located at the least point on the potential energy state.

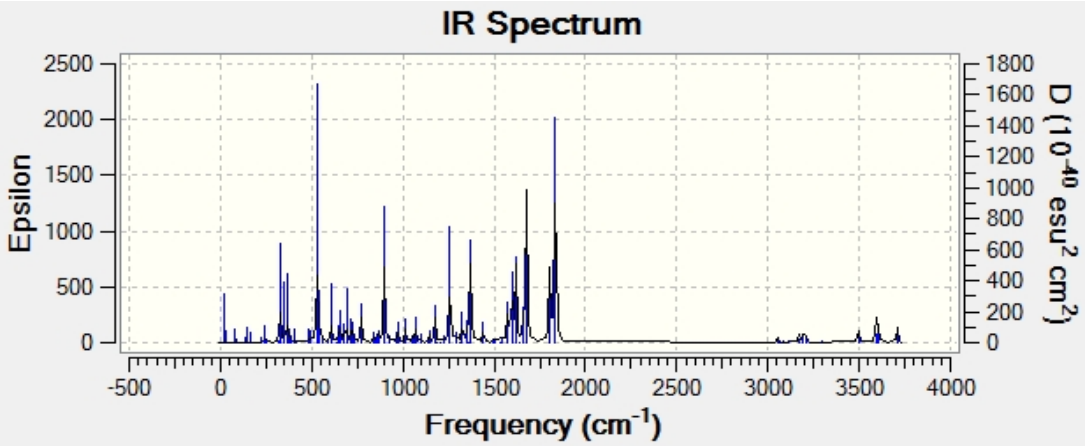

Figure 6. IR spectrum of PG with B3LYP/6-31G(d,p) basis set

Aromatic stretching vibrations

The aromatic C-H stretching frequencies show up in the range of 3100–3000 cm^{-1}. The ring C-C stretching vibrations occur in the range 1650–1400 cm^{-1}. In the present work, mode number 8 corresponds to the hypothetical aromatic C-H stretching vibrations. The PED% of the C-H vibration is 39% and 43% with a scaled frequency range of 3072 cm^{-1}. The aromatic C-C stretching vibrations are found in mode number 22, 33, 38, and 52 that appear in the fixed frequencies 1535, 1302, 1209, and 976 cm^{-1}.

Carbonyl group vibrations

The carbonyl stretching C=O vibration normally occurs in the range 1715-1680 cm^{-1}. The hypothetical extending vibrations were found in modes 15, 16 with high PED%. The scaled frequency at mode 16 with IR frequency of 1735 cm^{-1} corresponds to the pure C=O stretching with PED vibration of 88%.

N-H Stretching vibrations

The hypothetical N-H stretching is found in mode number 1-5; the PED% of N-H vibrations with scaled frequencies is computed in the range 3565-3361 cm^{-1}.

N-C Stretching vibrations

The determined N-C stretching vibrations are found in modes number 17, 21-30, 33, 35, 38, 44, 48, and 88, respectively, in the scaled frequencies 1613, 1556-1318, 1302, 1275, 1209, 1102, and 313 cm^{-1}.

Table 4. Vibrational wavenumbers of PG at B3LYP/6-31G(d,p) level of calculations

Mode No	Theoretical frequencies (cm^{-1})		Vibrational assignments PED ≥ 10%
	Unscaled frequency	Scaled frequency	
1	3709	3565.833	$\nu_{asN7H(7b)}$ (53%) + $\nu_{asN7H(7a)}$ (46%)
2	3601	3462.001	ν_{N2H2} (92%)
3	3594	3455.272	$\nu_{asN15H(15b)}$ (66%) + $\nu_{asN15H(15a)}$ (34%)
4	3591	3452.387	$\nu_{sN7H(7b)}$ (50%) + $\nu_{sN7H(7a)}$ (43%)
5	3496	3361.054	$\nu_{sN15H(15b)}$ (34%) + $\nu_{sN15H(15a)}$ (66%)
8	3195	3071.673	ν_{C19H19} (39%) + ν_{C21H21} (43%)
15	1836	1765.13	ν_{C3O8} (74%) + β_{C3N2C1} (12%)
16	1805	1735.327	ν_{C12O13} (88%)
17	1678	1613.229	ν_{N6C1} (12%) + ν_{N7C1} (10%) + $\beta_{H(15b)N15H(15a)}$ (27%) + $\beta_{H(7b)N7H(7a)}$ (28%)
18	1663	1598.808	$\beta_{H(15a)N15H(15b)}$ (41%) + $\beta_{H(7b)N7H(7a)}$ (28%)
21	1618	1555.545	ν_{N6C1} (38%) + $\beta_{H(7a)N7C1}$ (11%) + $\beta_{H(7a)N7H(7b)}$ (16%)
22	1597	1535.356	ν_{N9C10} (11%) + ν_{C4C5}(32%) + ν_{N6C5} (17%)
23	1575	1514.205	ν_{N9C10} (57%)
28	1441	1385.377	ν_{C4C5} (13%) + ν_{N2C1} (14%) + ν_{N11C5} (11%) + β_{N6C5C4} (14%) + β_{N9C4C5} (16%)
30	1371	1318.079	ν_{N11C5} (15%) + ν_{N11C12} (10%)
31	1365	1312.31	$\beta_{H(16b)C16C17}$ (17%)
33	1354	1301.736	ν_{C4C5} (12%) + ν_{N6C5} (16%) + ν_{N9C4} (33%) + $\beta_{H10C10N9}$ (10%)
35	1326	1274.816	ν_{N7C1} (18%) + β_{H2N2C1} (40%)
38	1258	1209.441	ν_{N11C12} (11%) + ν_{C12C14} (10%) + $\beta_{H10C10N9}$ (21%) + $\tau_{H14C14C12N11}$ (11%)
43	1175	1129.645	$\beta_{H(15b)N15C14}$ (18%) + $\beta_{H10C10N9}$ (10%) + $\beta_{H(16b)C16C17}$ (14%)
44	1146	1101.764	ν_{N15C14} (13%) + $\beta_{H(16b)C16C17}$ (13%)
48	1069	1027.737	ν_{N2C3} (26%)
52	1015	975.821	ν_{C14C16} (21%) + $\tau_{(H16b)C16C17C22}$ (10%)
54	971	933.5194	$\tau_{H22C22C17C16}$ (14%) + $\tau_{H19C19C18C17}$ (11%)
57	898	863.3372	$\beta_{H(15a)N15H(15b)}$ (12%) + $\tau_{(H16b)N15C14C12}$ (14%) + $\tau_{(H16a)N15C14C12}$ (32%)
63	772	742.2008	$\tau_{H20C20C21C22}$ (11%) + $\tau_{H19C19C18C17}$ (16%) + $\tau_{H21C21C20C19}$ (11%) + $\tau_{C17C18C19C20}$ (10%)
64	770	740.278	$\tau_{C10N9C4C5}$ (15%) + $\gamma_{O8N2C4C3}$ (43%) + $\gamma_{N6N11C5C4}$ (17%)
67	725	697.015	$\beta_{C10N9C4}$ (16%)
68	716	688.3624	$\tau_{H20C20C21C22}$ (26%) + $\tau_{C17C18C19C20}$ (16%) + $\gamma_{C16C21C18C17}$ (15%)

69	691	664.3274	$\tau_{H2N2C1N7}$ (21%) + $\tau_{C10N9C4C5}$ (13%) + $\gamma_{O8N2C4C3}$ (16%) + $\gamma_{N7N2N6C1}$ (11%) + $\gamma_{N6N11C4C5}$ (11%)
70	677	650.8678	β_{N2C1N6} (12%) + β_{N9C4C5} (18%)
71	656	630.6784	$\tau_{C10N9C4C5}$ (13%)
74	606	582.6084	$\tau_{H2N2C1N7}$ (61%)
77	545	523.963	$\tau_{(H7b)N7C1N2}$ (10%)
78	529	508.5806	$\tau_{(H7a)N7C1N2}$ (12%) + $\tau_{(H7b)N7C1N2}$ (61%)
85	368	353.7952	β_{N7C1N6} (13%) + $\beta_{C16C17C18}$ (14%) + $\tau_{(H15b)N15C14C16}$ (12%)
86	353	339.3742	β_{N7C1N6} (17%) + $\tau_{(H15b)N15C14C16}$ (26%) + $\tau_{(H15a)N15C14C16}$ (11%)
87	327	314.3778	β_{O8C3N2} (13%) + β_{O8C3N2} (15%) + β_{N7C1N6} (15%) + $\tau_{(H7a)N7C1N2}$ (22%) + $\tau_{(H7a)N7C1N2}$ (41%)
88	326	313.4164	ν_{N7C1} (18%) + β_{H2N2C1} (40%)

ν_{as} – asymmetric stretching vibration; ν_s – symmetric stretching vibration; β – bending vibration; τ – torsion; γ – out – of – plane bending.

3.3. ^{1}H and ^{13}C NMR spectra examination of PG

NMR spectroscopy is the way to uncover the conformational examination of natural atoms. Great quality calculations should be thought about for the quantum computation of unquestionably the isotropic attractive safeguarding tensors to yield more dependable outcomes. There are many reports on NMR isotropic attractive protecting tensor computations utilizing the GIAO technique related to the Density Function Theory (DFT). The GIAO 1H and 13C NMR chemical shift computations of PG are made in chloroform [scrf= (solvent=chloroform)] by utilizing the B3LYP/6-31G (d, p) basis set. The computational 1H and 13C NMR compound moves by DFT technique are displayed in **Table 5**.

Table 5. ^{1}H and ^{13}C NMR of PG (B3LYP/6-31G (d,p) basis set)

Proton	Chemical shifts (ppm)	Carbon	Chemical shifts (ppm)
H(10)	8.59	C12	182.6
H(2)	8.15	C3	161.3
H(21)	7.92	C1	158.8
H(19)	7.90	C5	155.7
H(22)	7.85	C17	146.6
H(20)	7.81	C10	143.9
H(18)	7.69	C22	135.3
H(7A)	4.47	C18	135.2
H(7B)	4.41	C21	135.1
H(14)	3.97	C19	132.8
H(16B)	3.81	C20	132.4
H(16A)	3.16	C4	127.5
H(15A)	2.97	C14	70.4
H(15B)	1.04	C16	42.9

3.4. Polarizability computations

The computed values of the dipole moment (μ), the polarizability (α_o), and the first hyperloarizability (β_{tot}) by the limited field approach are given in **Table 6** alone with the corresponding components. The dipole moment (μ) of PG is determined to be 3.18, respectively. The calculated polarizabilities α_{ij} have non-zero values and are dominated by the diagonal components. The calculated first hyperpolarizabilities PG is found to be 256.93 x 10^{-33} esu. Delocalization of charges, specifically headings, is demonstrated by large values of those specific

components of polarizability and hyperpolarizability. The main request hyperpolarizability is overwhelmed by β_{xxx} and β_{xxz} values. This shows that the delocalization of the charges in the presence of an outer field is supported toward those paths.

Table 6. The electric dipole moment μ (D), the mean polarizability (α) (10^{-24} esu) and the hyperpolarizability β_{tot} (10^{-33} esu) by DFT method of PG

Parameter	Value	Parameter	Value
μ_x	-2.1892	β_{xxx}	-346.3255
μ_y	2.2856	β_{xxy}	-14.9045
μ_z	0.3212	β_{xyy}	135.3217
μ	**3.1812**	β_{yyy}	18.8703
α_{xx}	254.9923	β_{xxz}	-2.6881
α_{xy}	1.9623	β_{xyz}	3.2414
α_{yy}	221.3252	β_{yyz}	-18.8494
α_{xz}	-3.3019	β_{xzz}	-35.8824
α_{yz}	-3.1.8759	β_{yzz}	6.5224
α_{zz}	92.2265	β_{zzz}	-48.8240
<α>	**189.5275**	**β_{tot}**	**256.9310**

α: 1a.u = $0.1482*10^{-24}$ esu ; β: 1a.u = $8.6393*10^{-33}$ esu.

3.5. Natural bond orbital examination

The natural bond orbital (NBO) examination of the compound PG is performed at B3LYP/6–31G (d, p) level of calculation. The donor bonding orbitals (BD), the acceptor antibonding orbitals (BD*), and the donor lone pair atoms (LP) are given in **Table 7** along with the E(2) values, which assess the interaction between the donor (filled) and acceptor (vacant) orbitals. The E(2) energy is the lowering energy that occurs during the hyper-conjugative electron transfer process, and thus E(2) can be referred to as stabilization energy. Larger the E(2) values, greater is the stability of the molecule. In the NBO analysis of the compound PG, the E(2) values are greater for the delocalization of the electrons between the bonds present in the guanine ring. The lone pair of electrons present in the nitrogen atom N2 is delocalized to C1-N6 and C3-O8 antibonding orbitals, and furthermore, N11 is delocalized to C4-C5 and C12-O13 antibonding orbitals.

Table 7. Second order perturbation theory analysis of fock matrix in NBO basis for PG

Donor NBO	Occupancy	Acceptor NBO	Occupancy	E(2) in kcal/mol
(BD)C17-C18	3.63	C19-C20	0.34667	21.56
(BD)C22-C21	3.65	C17-C18	0.36976	21.71
(BD)C19-C20	3.64	C22-C21	0.34634	21.36
(BD)C4-C5	3.69	C3-O8	0.32533	28.99
(BD)C1-N6	3.83	C4-C5	0.43893	20.58
(BD)C17-C18	3.63	C22-C21	0.34634	19.16
(BD)C22-C21	3.65	C19-C20	0.34667	19.40
(BD)C19-C20	3.64	C17-C18	0.36976	19.44
(BD)C10-N9	3.88	C4-C5	0.43893	15.61
(BD)C4-C5	3.69	C10-N9	0.28193	17.29
(BD)C4-C5	3.69	C3-O8	0.32533	28.99
(LP)O13	3.86	C14-C12	0.06630	17.90
(LP)O13	3.85	C12-N11	0.10254	30.83
(LP)N11	1.57	C12-O13	0.12377	21.98
(LP) N11	1.57	C4-C5	0.43893	37.12
(LP)O8	3.82	C4-C3	0.06264	19.07
(LP)O8	3.82	C3-N2	0.10249	33.02
(LP)N2	1.65	C3-O8	0.32533	38.11

(LP)N2	1.65	C1-N6	0.42020	58.15
(LP)N7	1.83	C1-N6	0.42020	30.95

3.6. Atoms in molecule analysis

The molecule PG is subjected to AIM analysis, and it exposed 41 bond critical points (displayed in orange colour) with a (3, -1) topology between the covalently bonded atoms and 6 ring critical points (RCP) displayed in yellow colour with a (3, +1) topology within the ring, and it is pictured out in **Figure 7** using a multifunctional wavefunction analyzer 'Multiwfn'. The values of electron densities (ρ), laplacian of electron density ($\nabla^2\rho_{BCP}$), bond ellipticity (ε), the three eigen values (λ_1, λ_2, λ_3), the relationship between the largest curvature of the charge density perpendicular and parallel to the bond path ($|\lambda_1|/\lambda_3$), the potential energy density (V), the kinetic energy density (G), the kinetic energy density per charge unit (G/ρ_{BCP}) values, and the delocalization index (DI) for the bond critical points (BCP) and ring critical point (RCP) present in the molecule PG are tabulated in **Table 8**.

The electron densities (ρ_{BCP}) at BCPs forming a part of the benzene rings C17-C22, C18-C17, C22-C21, C19-C20, C18-C19, and C20-C21 are ranging from 0.254 to 0.313 a.u. The electron densities (ρ_{BCP}) at BCPs forming a part of the guanine ring C10-N11, N9-C10, C5-N11, C4-N9, C4-C5, N6-C5, C3-C4, O8-C3, N2-C3, C1-N6 N2-C1, and N7-C1 range from 0.292 to 0.411; the ρ_{BCP} at BCPs constituting the carbons C14-C16, C12-C14, and C16-17 ranges from 0.230 to 0.254; and the ρ_{BCP} at C12-O13 and O8-C3 BCP is 0.412 and 0.411, respectively.

The higher electron density at BCP C12-O13 and O8-C3 indicated the presence of strong interaction between the atoms C12 and O13 and O8-C3. The bond ellipticity values for the BCPs at the benzene ring and guanine ring (0.205–0.335) are indicating a higher π bond interaction in the benzene ring and guanine ring. The BCP C12-O13 and O8-C3 have ellipticity values of 0.108 and 0.119, indicating stronger π-bond interactions between the atoms C12-O13 and O8-C3 than all other BCPs.

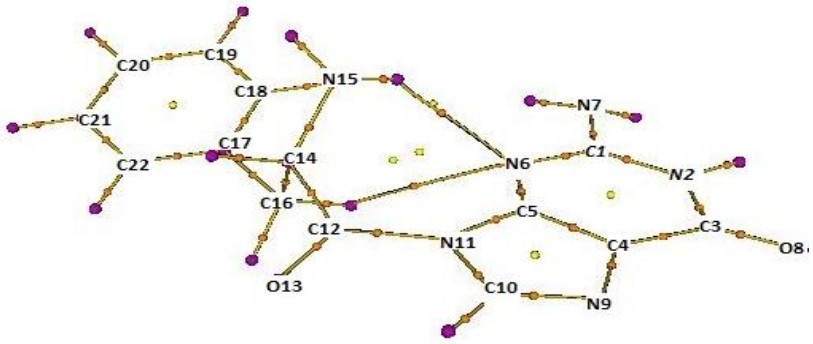

Figure 7. BCPs (displayed in orange colour) and RCPs (displayed in yellow colour) using multiwave functionlizer

The $|\lambda 1|/\lambda 3$ values are greater than 1 for all BCPs except the BCP C12-O13 and O8-C3. C11-O13 and O8-C3 BCP have $|\lambda 1|/\lambda 3$ less than 1. The G/ρ_{BCP} value greater than 1 indicates strong interaction between the bonded atoms. The DI of all the BCPs in the molecule PG are nearer to 1 or greater than 1 because the average number of electrons shared between the interacting atoms is higher in all the BCPs and the electrons are not localized to any one of the interacting atoms as in the case of atoms constituting hydrogen bonds. The AIM analysis has predicted that the lone pair of electrons of oxygen atoms O13 and O8 is not involved in any hydrogen bonding in the molecule, and it is visualized using multiwavefunction analyzer **Figure 8**. The atom N15 has two extra intramolecular bonds between N15's hydrogen with N6 and N15 with the C18 carbon atom. Apart from that, N15, C16's hydrogen is involved in new intramolecular bonding with N6. This AIM analysis confirms three new intramolecular bonding and two new RCP in PG molecule.

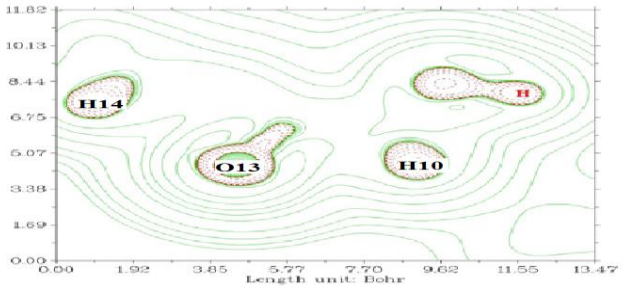

Figure 8. Contour map of PG depicting $\nabla^2\rho$ in PG [green – positive region; red – negative region]

Table 8. Topological properties at the BCP's and RCP's by AIM analysis

BCP	**ρ**	**$\nabla^2\rho$**	**ε**	**$l\lambda_1 l/\lambda_3$**	**DI**	**V**	**G**	**G/ρ**
N15-H15b	0.341	-1.75	0.05	1.821	0.842	-0.559	0.061	0.179
N15-C14	0.275	-0.769	0.058	1.693	1.008	-0.404	0.106	0.385
C14-C16	0.23	-0.488	0.025	1.215	0.911	-0.229	0.054	0.235
C12-C14	0.254	-0.621	0.054	1.385	0.875	-0.271	0.058	0.228
C16-C17	0.254	-0.598	0.034	1.37	0.996	-0.268	0.059	0.232
C17-C22	0.309	-0.829	0.209	1.877	1.353	-0.403	0.098	0.317
C12-O13	0.412	0.191	0.108	0.482	1.311	-1.459	0.753	1.828
C18-C17	0.309	-0.83	0.212	1.881	0.037	-0.404	0.098	0.317
C22-C21	0.313	-0.854	0.216	1.948	1.399	-0.413	0.099	0.316
N6-H16b	0.01	0.032	0.131	0.19	0.041	-0.006	0.007	0.700
C19-C20	0.312	-0.854	0.214	1.947	1.395	-0.412	0.099	0.317
C18-C19	0.312	-0.849	0.217	1.939	1.392	-0.411	0.099	0.317
C20-C21	0.312	-0.852	0.211	1.938	1.386	-0.411	0.099	0.317
N11-C12	0.279	-0.849	0.044	2.01	0.87	-0.508	0.148	0.530
C10-N11	0.292	-0.801	0.143	1.938	0.952	-0.669	0.234	0.801
N9-C10	0.378	-1.031	0.335	1.652	1.416	-1.051	0.396	1.048
C5-C11	0.298	-0.864	0.156	2.136	0.99	-0.664	0.224	0.752
C4-N9	0.318	-1.019	0.129	2.725	1.147	-0.613	0.179	0.563
C4-C5	0.322	-0.889	0.322	2.078	1.259	-0.449	0.133	0.413
N6-C5	0.332	-1.141	0.14	3.119	1.122	-0.683	0.199	0.599
C3-C4	0.294	-0.797	0.205	1.748	1.04	-0.355	0.078	0.265
O8-C3	0.411	0.027	0.119	0.521	10269	-1.421	0.714	1.737
N2-C3	0.272	-0.783	0.074	1.912	0.857	-0.524	0.164	0.603
C1-N6	0.368	-1.312	0.242	3.569	1.223	-0.857	0.264	0.717
N2-C1	0.324	-1.059	0.176	2.556	1.002	-0.736	0.235	0.725
N6-H15b	0.021	0.062	0.032	0.22	0.002	-0.015	0.015	0.714
N7-C1	0.325	-1.145	0.182	3.055	0.998	-0.662	0.188	0.578
RCP	**ρ**	**$\nabla^2\rho$**		**$l\lambda_1 l/\lambda_3$**		**V**	**G**	**G/ρ**
N15-C14-C16-H16b-N6-H15b	0.007	0.029	-	0.137	-	-0.005	0.006	0.857
N15-C14-C12-N11-C5-N6-H15b	0.007	0.035	-	0.061	-	-0.005	0.007	1.00
C17-C18-C19-C20-C21-C22	0.02	0.162	-	0.163	-	-0.022	0.031	1.55
N11-C10-N9-C4-C5	0.052	0.405	-	0.244	-	-0.077	0.089	1.711

C4-C3-N2-C1-N6-C5	0.021	0.165	-	0.143	-	-0.023	0.032	1.524
C16-H16b-N6-C1-N7-H7b-H18-C18-C17	0.001	0.004	-	0.168	-	-0.0003	0.0006	0.600

3.7. Electrochemistry of PG

The anionic form of the molecule PG is optimized at B3LYP / 6–31G+ (d,p) level of computation, and the selected geometrical parameters like the bond length and the torsional angles that govern the rotation of the four rotatable bonds N11-C12, C12-C14, C14-C16, and C16-C17 of the molecule in anionic form are compared with the geometrical parameters of the molecule PG in the neutral form **Table 9**. In the anionic form of the molecule, the bond lengths of C1-N7, C3-O8, C12-O13, and N11-C12 bonds are slightly varied from the C1-N7, C3-O8, C12-O13, and N11-C12 bond lengths in the neutral molecule.

The elongation of the C12-O13 and N11-C12 bonds is well explained by the NBO analysis of the anionic form of the molecule PG. The NBOs of the neutral molecule and anion of PG are analyzed. The hybridizations of the atoms involved in the formation of the vital bonds present in the guanine and phenylalanine rings are analyzed. The hybridizations underwent by the atoms involved in the formation of the vital bonds in the neutral and anionic forms of the molecule PG involved are presented in **Table 10**, which consists of the bond length of the bonds presented. The hybridization of the C12, O13, and N11 in the formation of the C12–O13 and C12–N11 appears to be unperturbed in the anionic form of the molecule. Hence there is some significant change in the bond length.

Table 9. Selected geometric parameters of the anionic and neutral forms of the molecule PG

Bond length (Å)	**Neutral**	**Anion**
C1-N7	1.372	1.401
C3-O8	1.216	1.234
N11-C12	1.433	1.409
C12-O13	1.213	1.254
C12-O14	1.529	1.520
C14-N15	1.457	1.467
C14-C16	1.564	1.576
C16-C17	1.511	1.507
Torsion angle(º)	**Neutral**	**Anion**
O13-C12-N11-C10	-11.743	-4.407
013-C12-C14-N15	132.567	129.351
N11-C12-C14-C16	85.367	74.529
C12-C14-C16-C17	167.220	167.937
C14-C16-C17-C22	89.233	96.267
C14-C16-C17-C18	-88.70	-81.817

Table 10. Natural bond hybridisation calculated for vital bonds by NBO analysis for PG

Bond	**Bonded atoms**	**Neutral form**				**Anion form**			
		Hybridisation			**Bond length (A^O)**	**Hybridisation**			**Bond length (A^O)**
N15-C14	N15		$sp^{2.29}$		1.479		$sp^{2.28}$		1.467
	C14		$sp^{3.27}$				$sp^{2.98}$		
C14-C16	C14		$sp^{2.55}$		1.536		$sp^{2.66}$		1.576
	C16		$sp^{2.77}$				$sp^{3.01}$		

C14-C12	C14		sp^3		1.53		$sp^{3.06}$		1.520
	C12		$sp^{1.49}$				$sp^{1.59}$		
C16-C17	C16		$sp^{2.57}$		1.496		$sp^{2.67}$		1.507
	C17		$sp^{2.18}$				$sp^{2.11}$		
C12-O13	C12	$sp^{2.19}$		s^0p^1	1.213		$sp^{2.05}$		1.254
	O13	$sp^{1.34}$		s^0p^1			$sp^{1.37}$		
C12-N11	C12		$sp^{2.52}$		1.458	$sp^{2.47}$		s^0p^1	1.409
	N11		$sp^{1.96}$			$sp^{1.86}$		s^0p^1	
N11-C10	N11		$sp^{2.11}$		1.43		$sp^{2.24}$		1.141
	C10		$sp^{2.54}$				$sp^{2.52}$		
N11-C5	N11		$sp^{1.94}$		1.411		$sp^{1.92}$		1.403
	C5		$sp^{2.44}$				$sp^{2.60}$		
C10-N9	C10	$sp^{1.98}$		s^0p^1	1.333	$sp^{1.86}$		s^0p^1	1.312
	N9	$sp^{1.85}$		s^0p^1		$sp^{1.78}$		s^0p^1	
N9-C4	N9		$sp^{2.17}$		1.404		$sp^{2.26}$		1.372
	C4		$sp^{2.31}$				$sp^{2.21}$		
C4-C3	C4		$sp^{1.78}$		1.445		$sp^{1.88}$		1.429
	C3		$sp^{1.49}$				$sp^{1.56}$		
C4-C5	C4	$sp^{1.97}$		s^0p^1	1.399	$sp^{1.94}$		s^0p^1	1.417
	C5	$sp^{1.65}$		s^0p^1		$sp^{1.63}$		s^0p^1	
C3-O8	C3	$sp^{1.98}$		s^0p^1	1.215	$sp^{1.89}$		s^0p^1	1.234
	O8	$sp^{1.41}$		s^0p^1		$sp^{1.43}$		s^0p^1	
C3-N2	C3		$sp^{2.82}$		1.455		$sp^{2.79}$		1.434
	N2		$sp^{1.81}$				$sp^{1.90}$		
N2-H2	N2		$sp^{2.32}$		0.998		$sp^{2.51}$		1.011
	H2		sp^0				sp^0		
N2-C1	N2		$sp^{1.92}$		1.409		$sp^{1.71}$		1.382
	C1		$sp^{2.03}$				$sp^{2.11}$		
C1-N7	C1		$sp^{2.19}$		1.421		$sp^{2.12}$		1.401
	N7		$sp^{2.03}$				$Sp^{1.88}$		
C1-N6	C1	$sp^{1.81}$		s^0p^1	1.342	$sp^{1.80}$		s^0p^1	1.311
	N6	$sp^{1.81}$		s^0p^1		$sp^{1.83}$		s^0p^1	
N7-H7(A)	N7		$sp^{2.93}$		0.996		$sp^{2.81}$		1.025
	H7(A)		sp^0				sp^0		
N7-H7(B)	N7		$sp^{2.58}$		0.996		$sp^{2.72}$		1.015
	H7(B)		sp^0				sp^0		
N6-C5	N5		sp^2		1.396		$sp^{1.94}$		1.358
	C5		$sp^{2.02}$				$sp^{1.94}$		

3.8. Electrophilicity index of PG

The determination of various global and local reactivity descriptors in the context of chemical reactivity is also performed, and the electrophilicity at the site of PG is revealed. The local reactivity descriptors like fukui functions and dual descriptors are calculated employing Mulliken population (MCA), natural population (NCA), and Hirshfeld population (HCA), and independent single point energy calculations have been made on N-1, N and N+1 electronic systems (where N = 156, the total number of electrons in PG) with the same molecular geometry (devoid of any structural changes in the N-1, N and N+1 electronic systems) at B3LYP / 6 – 31G+ (d, p) level.
The Mulliken charge, natural charge, and Hirshfeld charge on the atoms pictured out in **Figure 9** are from the DFT analysis of the molecule PG and its N+1 and N-1 electronic forms and are used to determine the f_k^+ and f_k^- values. The f_k^+ and f_k^- values are determined for all the vital atomic sites based on mulliken charges (MCA), natural charges (NCA), and hirshfeld charges (HCA). The dual descriptor (Δf) is calculated for atoms forming the sites for attack from the f_k^+ and f_k^- values. The

q_k^N, q_k^{N+1}, q_k^{N-1}, f_k^+, f_k^-, and Δf values for the vital atomic sites are given in **Table 11**. The NCA and HCA schemes provide a positive Δf value for the N6 and N15 atomic sites, indicating that they are favorable for nucleophilic attack, and a negative Δf value for the C12 atomic site, indicating that the atomic site is favorable for electrophilic attack.

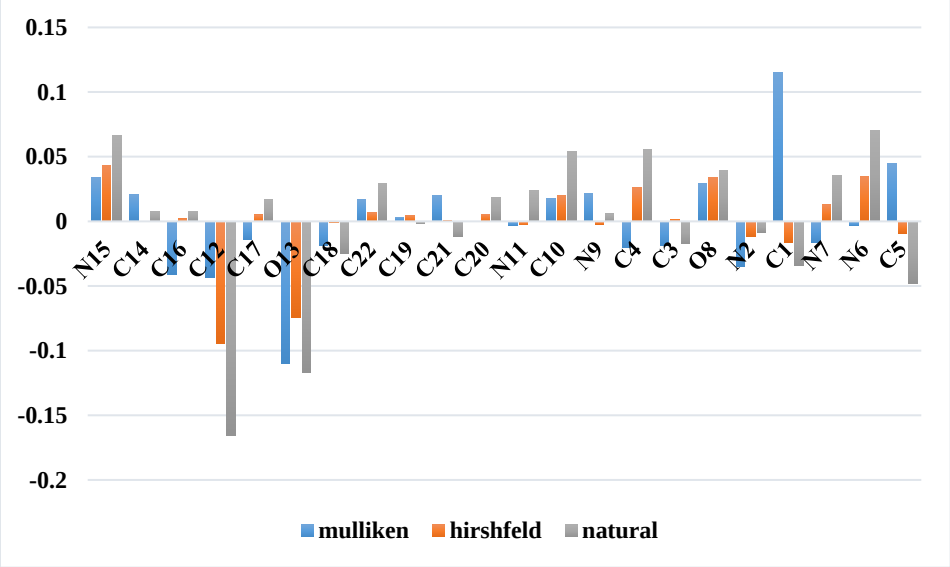

Figure 9. Mulliken, Hirshfeld and Natural changes in PG

Table 11. Fukui functions, dual descriptor and local electrophilicity at vital atomic sites based on Mulliken charges (MCA), Natural charges (NCA) and Hirshfeld charges (HCA) for PG

Mulliken charge based analysis (MCA):

Atomic site	q^N	q^{N+1}	q^{N-1}	f_k^-	f_k^+	Δf
N15	-0.0891	-0.1435	-0.0008	-0.0882	-0.0544	0.0338
C14	0.1004	0.0913	0.1301	-0.0297	-0.0091	0.0207
C16	-0.0069	-0.0577	0.0028	-0.0097	-0.0508	-0.0411
C12	0.5892	0.5092	0.6260	-0.0368	-0.0800	-0.0432
C17	0.1242	0.1116	0.1228	0.0015	-0.0126	-0.0141
O13	-0.4310	-0.5657	-0.4066	-0.0244	-0.1347	**-0.1103**
C18	-0.0551	-0.0719	-0.0573	0.0022	-0.0168	-0.0190
C22	-0.0348	-0.0648	0.0122	-0.0470	-0.0300	0.0170
C19	0.0019	-0.0442	0.0514	-0.0495	-0.0461	0.0034
C21	-0.0002	-0.0333	0.0531	-0.0533	-0.0331	0.0202
C20	0.0034	-0.0589	0.0659	-0.0625	-0.0623	0.0002
N11	-0.5817	-0.5628	-0.6039	0.0222	0.0189	-0.0033
C10	0.4522	0.3499	0.5723	-0.1201	-0.1024	0.0177
N9	-0.4993	-0.5314	-0.4454	-0.0539	-0.0321	0.0218
C4	0.1425	0.0987	0.1662	-0.0237	-0.0438	-0.0200
C3	0.5835	0.5322	0.6160	-0.0325	-0.0513	-0.0188
O8	-0.4910	-0.5513	-0.4018	-0.0893	-0.0603	0.0290
N2	-0.3218	-0.3833	-0.2953	-0.0265	-0.0615	-0.0350
C1	0.6499	0.6618	0.7533	-0.1034	0.0120	**0.1154**
N7	-0.0590	-0.1594	0.0252	-0.0842	-0.1004	-0.0162
N6	-0.5983	-0.6121	-0.5877	-0.0106	-0.0138	-0.0032
C5	0.5211	0.4858	0.6014	-0.0803	-0.0353	0.0450

Natural charge based analysis (NCA):

Atomic site	q^N	q^{N+1}	q^{N-1}	f_k^-	f_k^+	Δf
N15	-0.9015	-0.9123	-0.8239	-0.0776	-0.0108	0.0668
C14	-0.1456	-0.1304	-0.1532	0.0076	0.0153	0.0077

C16	-0.4998	-0.4973	-0.4944	-0.0054	0.0025	0.0079
C12	0.7503	0.5939	0.7412	0.0091	-0.1564	**-0.1655**
C17	-0.0384	-0.0420	-0.0181	-0.0203	-0.0037	0.0166
O13	-0.5335	-0.6799	-0.5037	-0.0298	-0.1464	-0.1165
C18	-0.2318	-0.2421	-0.2460	0.0142	-0.0103	-0.0246
C22	-0.2430	-0.2555	-0.2009	-0.0421	-0.0125	0.0295
C19	-0.2277	-0.2547	-0.2024	-0.0252	-0.0270	-0.0018
C21	-0.2249	-0.2379	-0.2234	-0.0015	-0.0130	-0.0115
C20	-0.2439	-0.2840	-0.1854	-0.0584	-0.0401	0.0183
N11	-0.4699	-0.4474	-0.4688	-0.0011	0.0225	0.0236
C10	0.2125	0.1641	0.3147	-0.1022	-0.0484	0.0538
N9	-0.4397	-0.4782	-0.3951	-0.0446	-0.0386	0.0060
C4	-0.0382	-0.0803	0.0595	-0.0977	-0.0421	0.0556
C3	0.6584	0.6483	0.6511	0.0073	-0.0100	-0.0173
O8	-0.5770	-0.6459	-0.4687	-0.1083	-0.0690	0.0394
N2	-0.6602	-0.6838	-0.6449	-0.0152	-0.0236	-0.0084
C1	0.6443	0.5850	0.6695	-0.0251	-0.0593	-0.0342
N7	-0.8512	-0.8741	-0.7926	-0.0586	-0.0229	0.0357
N6	-0.6154	-0.6089	-0.5513	-0.0641	0.0065	**0.0706**
C5	0.3727	0.2961	0.4011	-0.0284	-0.0766	-0.0482

Hirshfeld charge analysis (HCA):

Atomic site	q^{N}	q^{N+1}	q^{N-1}	f_k^-	f_k^+	**Δf**
N15	-0.2191	-0.2306	-0.1643	-0.0548	-0.0114	**0.0434**
C14	0.0193	0.0091	0.0293	-0.0099	-0.0102	-0.0003
C16	-0.0575	-0.0668	-0.0461	-0.0114	-0.0093	0.0021
C12	0.1960	0.0921	0.2055	-0.0095	-0.1039	**-0.0944**
C17	-0.0006	-0.0093	0.0131	-0.0137	-0.0087	0.0050
O13	-0.2378	-0.3553	-0.1945	-0.0433	-0.1175	-0.0742
C18	-0.0509	-0.0584	-0.0446	-0.0064	-0.0074	-0.0011
C22	-0.0444	-0.0633	-0.0185	-0.0259	-0.0189	0.0070
C19	-0.0449	-0.0693	-0.0158	-0.0291	-0.0244	0.0047
C21	-0.0405	-0.0617	-0.0184	-0.0220	-0.0212	0.0008
C20	-0.0438	-0.0803	-0.0018	-0.0421	-0.0364	0.0056
N11	-0.0056	-0.0191	0.0052	-0.0108	-0.0136	-0.0028
C10	0.0600	0.0103	0.1294	-0.0695	-0.0497	0.0198
N9	-0.1679	-0.2192	-0.1188	-0.0491	-0.0514	-0.0023
C4	-0.0275	-0.0671	0.0382	-0.0657	-0.0396	0.0261
C3	0.1509	0.1238	0.1791	-0.0283	-0.0270	0.0012
O8	-0.2880	-0.3458	-0.1959	-0.0921	-0.0578	0.0343
N2	-0.0640	-0.0932	-0.0465	-0.0175	-0.0292	-0.0117
C1	0.1581	0.1101	0.1900	-0.0318	-0.0480	-0.0162
N7	-0.1495	-0.1845	-0.1017	-0.0478	-0.0350	0.0128
N6	-0.1840	-0.1945	-0.1390	-0.0450	-0.0105	0.0344
C5	0.0707	0.0242	0.1080	-0.0373	-0.0465	-0.0092

3.9. Molecular electrostatic potential (MEP) surfaces

The reactive behavior of the molecule is visualized with the help of a three-dimensional MEP surface. The MEP surface is a superimposition of the electrostatic potential on the iso-electron density surface. MEP surface describes the charge distribution in the molecule and helps in predicting the sites for nucleophilic and electrophilic attack in the molecule. The MEP surface has been plotted for the molecule PG (**Figure 10**). The region of negative charge is pictured out in red,

and it is found around the electronegative N9, O13, and O8 in the molecule PG. The red colour region is to electrophilic attack. The blue colour region represents a strong positive region (N7, N6, and N15) and is prone to nucleophilic attack. The green colour region corresponds to a potential half-way between the two extremes of the red (-8.310 e^{-2}) and blue (+8.310 e^{-2}) regions. In PG C10 and the benzene ring of phenylalanine, there is a green region that has a potential attack of half nucleophilic and half electrophilic.

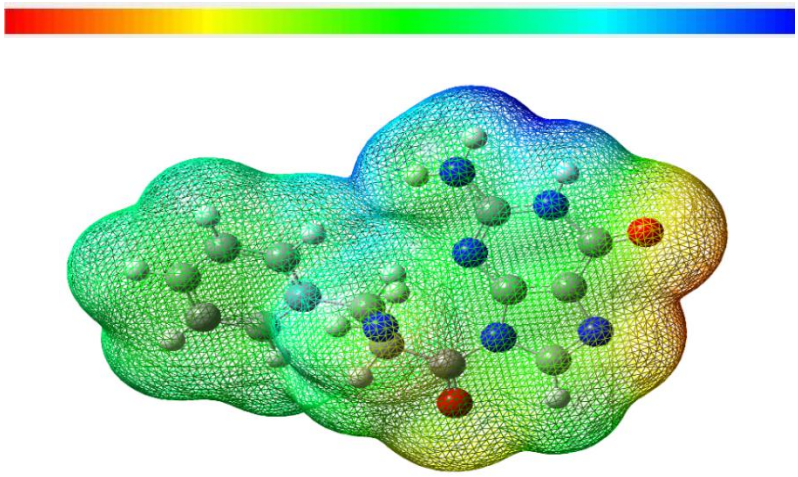

Figure 10. MEP surfaces of PG

3.10. HOMO-LUMO of PG

HOMO-LUMO pictures of molecule PG are introduced in **Figure 11**. The p_z orbitals of guanine iotas (C1, N2, C3, C4, C5, N6, N7, O8, N9, C10, and N11) and the atom of N15 in the phenylalanyl are included in the arrangement of the HOMO orbitals. The p_z orbitals of phenylalanyl carbon molecules and the H2 atom alone aren't included in the arrangement of the HOMO orbital. The LUMO orbital is observed as guanine for all molecules and phenylalanyl atoms except C20, N15's hydrogens, and benzene's hydrogen. C18 and C19 involved very minute-level formation of LUMO. The band gap between the HOMO and LUMO orbitals is 4.6134 eV.

A calculated chemical hardness (η), chemical softness (S), chemical potential (σ), electron negativity (χ), and globalphilicity (ω) of the molecule PG is given in **Table 12**. The molecule hardness was found to be 2.3067, indicating a relatively hard molecule, which is less reactive and more stable. In contrast, the molecule softness was 0.4335, suggesting a moderate level of reactivity. The chemical potential was calculated to be 3.7404, indicating a relatively high reactivity and tendency to form bonds with other molecules. The electronegativity was 1.4337, which is moderate and suggests a balanced tendency to attract and donate electrons. Finally, the globalphilicity was 3.0326, indicating a relatively high tendency to form bonds with other molecules. These molecular properties suggest that the optimized structure is a relatively stable molecule with moderate reactivity and a tendency to form bonds with other molecules. The results provide valuable insights into the molecular behavior and reactivity of the optimized structure, which can be useful for further experimental and theoretical studies.

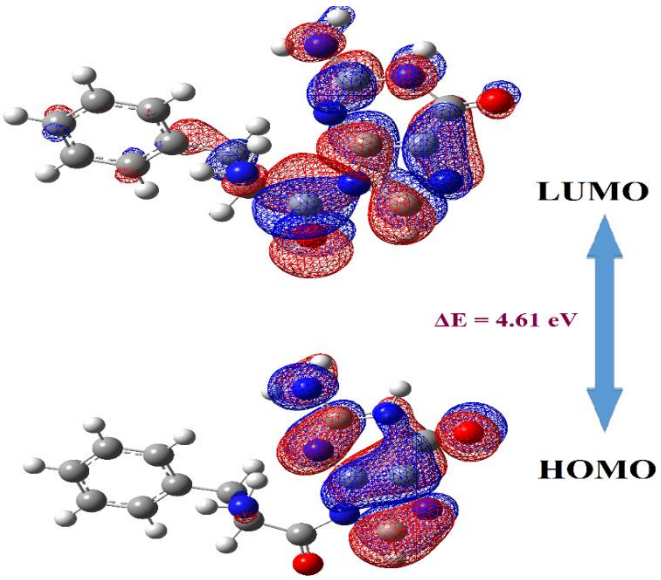

Figure 11. HOMO-LUMO Picture of PG

Table 12. Calculated Chemical hardness (η), Chemical softness (S), Chemical potential (σ), Electro negativity (χ) and globalphilicity (ω) of the molecule PG

HOMO (eV)	LUMO (eV)	Bandgap energy (eV)	η	S	σ	χ	ω
-6.0471	-1.4337	4.6134	2.3067	0.4335	3.7404	1.4337	3.0326

4. Conclusion

The stable conformer of PG is deduced by the DFT method. An optimized structure is subjected to IR frequency investigation; the theoretical value of PG is analyzed by means of potential energy distribution (PED%) calculation using the vibrational energy distribution analysis (VEDA) program. The value of NMR chemical shifts obtained by the DFT method. The PG is subjected to NBO analysis, and the stability of the molecule is examined. The electrochemical studies are computed by a computational study on the hybridization of vital bonds in the neutral and anionic forms of the molecule. On the basis of the Mulliken charge analysis (MCA), natural charge analysis (NCA), and Hirshfeld charge analysis (HCA), the fukui function is carried out to examine the local electrophilicity of crucial atomic sites in the molecule. The Fukui function calculation predicts N15 is the more nucleophilic attack site of the molecule, and C12 is the more electrophilic attack site of the molecule. The topological analysis (AIM) of the molecule predicts 3 new BCPs and 3 new RCPs. The band gap energy is found to be 4.61 eV. Overall, the molecular properties values suggest that the molecule is relatively hard, less reactive, and has a moderate electronegativity. However, it also has a relatively high chemical potential and globalphilicity, indicating a tendency to form bonds with other molecules.

References

[1] M. J. Berridge, “Inositol trisphosphate and calcium signalling mechanisms”, Biochimica et Biophysica Acta (BBA)-Molecular Cell Research, vol. 1793, **(2009)**, pp. 933.

[2] M. T. Kozinova, I. A. Demina, V. B. Krylov, I. I. Baskin I and M. P. Rubtsova, “Functional Analysis of the C-terminal Domain of the Human Protein Rpp30 Involved in ribonucleoprotein assembly”, Nucleic Acids Research, vol. 50, no. 8, **(2022)**, pp. 4574-4600.

[3] George M. Kapalka, “Nutritional and Herbal Therapies for Children and Adolescents”, **(2010)**, pp. 141-187.

[4] Gerald Litwack, “Metabolism of Amino Acids”, Human Biochemistry, vol. 13, **(2017)**, pp. 359-394.

[5] Generoso G. Gascon, Pinar T. Ozand, Bruce Cohen, "Aminoacidopathies and Organic Acidopathies, Mitochondrial Enzyme Defects, and Other Metabolic Errors", Textbook of Clinical Neurology, vol. 31, (**2007**), pp. 641-681.

[6] C. H. Lee, Y. H. Liu, C. H. Lin, T. C. Lin, M. J. Lai, T. C. Chen, H. C. Huang, C. C. Hsu, C. W. Chang, Y. Y. Chang, H. Y. Lin and C. C. Lai, "Design and synthesis of novel 9-(2-phenylethynyl)guanine derivatives as inhibitors of human telomerase", Bioorganic & Medicinal Chemistry Letters, vol. 17, no. 22, **(2007)**, pp. 6167-6172.

[7] J. Li, C. Han, Y. Xue, H. Yan and B. Yu, "Design, synthesis, and evaluation of novel guanine derivatives as inhibitors of human DNA polymerase α", Bioorganic & Medicinal Chemistry Letters, vol. 24, no. 14, **(2014)**, pp. 3128-3132. DOI: 10.1016/j.bmcl.2014.05.032.

[8] L. O. Klotz, X. Hou, C. Jacob and N. Buchner, "Guanine-based distinctive drug design: Novel targets for future antiviral and anticancer chemotherapy", Chem. Med. Chem., vol. 9, no. 9, **(2014)**, pp. 2021-2030.

[9] G. B. Elion, "Acyclovir: Discovery, Mechanism of Action, and Selectivity", Journal of Medical Virology, vol. 1, **(1993)**, pp. 2-6.

[10] G. B. Elion, P. A. Furman, J. A. Fyfe, Paulo de Miranda, Lilia Beauchamp and H. J. Schaeffer, "Selectivity of action of an antiherpetic agent, 9-(2-hydroxyethoxymethyl)guanine", Proc. Natl. Acad. Sci. USA Medical Sciences, vol. 74, no. 12, **(1977)**, pp. 5716-5720.

[11] Christian Gibert, Julie Bestman-Smith, Guy Boivin, "Resistance of herpesviruses to antiviral drugs: clinical impacts and molecular mechanisms", Drug Resistance Updates, vol. 5, **(2002)**, pp. 88-114.

[12] Lynne Strasfeld, Sunwen Chou, "Antiviral Drug Resistance: Mechanisms and Clinical Implications Antiviral", Drug Resistance, vol. 24, **(2010)**, pp. 413-437.

[13] J. Antona, Wagstaff, Diana Faulds and L. Karen, "Aciclovir A Reappraisal of its Antiviral Activity", Pharmacokinetic Properties and Therapeutic Efficacy Drugs, vol. 47, no. 1, **(1994)**, pp. 153-205.

[14] P. Vijaya and K. R. Sankaran, "A combined experimental and DFT study of novel unsymmetrical azine 2-(4-methoxybenzylidene)-1-(1-(4-isobutylphenyl)ethylidene) hydrazine", Spectrochimica Acta Part A: Molecular and Biomolecular Spectroscopy, vol. 138, **(2015)**, pp. 460-473.

[15] M. Elango, R. Parthasarathi, G. K. Narayanan, A. M. Sabeelullah, U. Sarkar, N. S. Venkatasubramanian, V. Subramanian, P. K. Chattaraj, "Molecule-in-a-box: how does confinement affect the electronic structure, stability, and reactivity of the encapsulated species", Journal of Chemical Sciences, vol. 117, no. 4, **(2005)**, pp. 369-378.

[16] T. Bhaskar, M. Shanmugasundari, P. Vijaya, N. Banumathi, "Synthesis of 2-(2-amino-1,3 – dihydroxypropane-2-ylamino)benzoic acid", Research Journal of Chemistry and Environment, vol. 26, no. 12, **(2022)**, pp. 146-153.

[17] T. Bhaskar , D. Gana Saraswathy, N. Banumathi, P. Vijaya, "Synthesis, Characterization and DFT study of 2-amino-2'(diphenylamino)- Propane-1,3-diol", Research Journal of Chemistry and Environment, vol. 27, no. 6, **(2023)** , pp. 74-79.

[18] R. F. Bader, "Atoms in Molecules: A Quantum Theory", Oxford University Press, Oxford, **(1990)**.